Supporting Information

Rapid screening by scanning electrochemical microscopy (SECM) of dopants for Bi_2WO_6

Improved photocatalytic water oxidation with Zn doping

Chinmoy Bhattacharya, Heung Chan Lee and Allen J. Bard*

Center for Electrochemistry, Department of Chemistry and Biochemistry, The University of Texas at Austin, 105 E 24th Street, Stop A5300, Austin, TX 78712

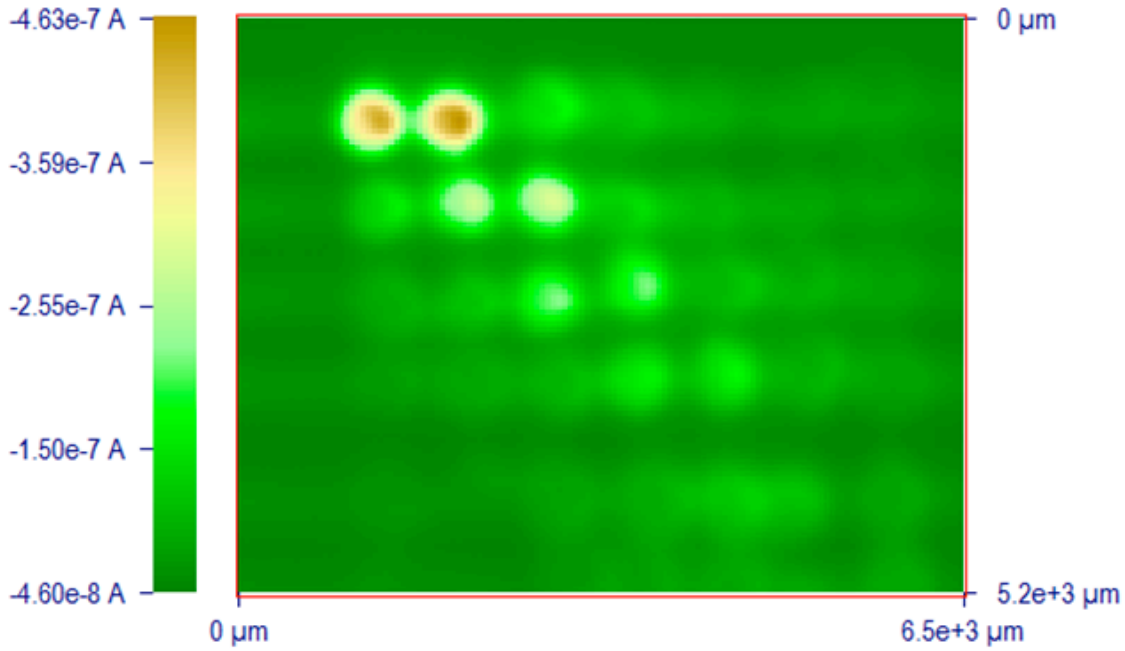

Figure S1. (a) SPECM images of the array photocurrent of Co and V doped Bi/W oxide photocatalyst in a 0.1 M Na_2SO_3/Na_2SO_4 solution with the array held at constant applied potential of 0.2 V (vs. Ag/AgCl reference electrode) under UV-visible light. The arrays show 'negative effect' of the dopants.

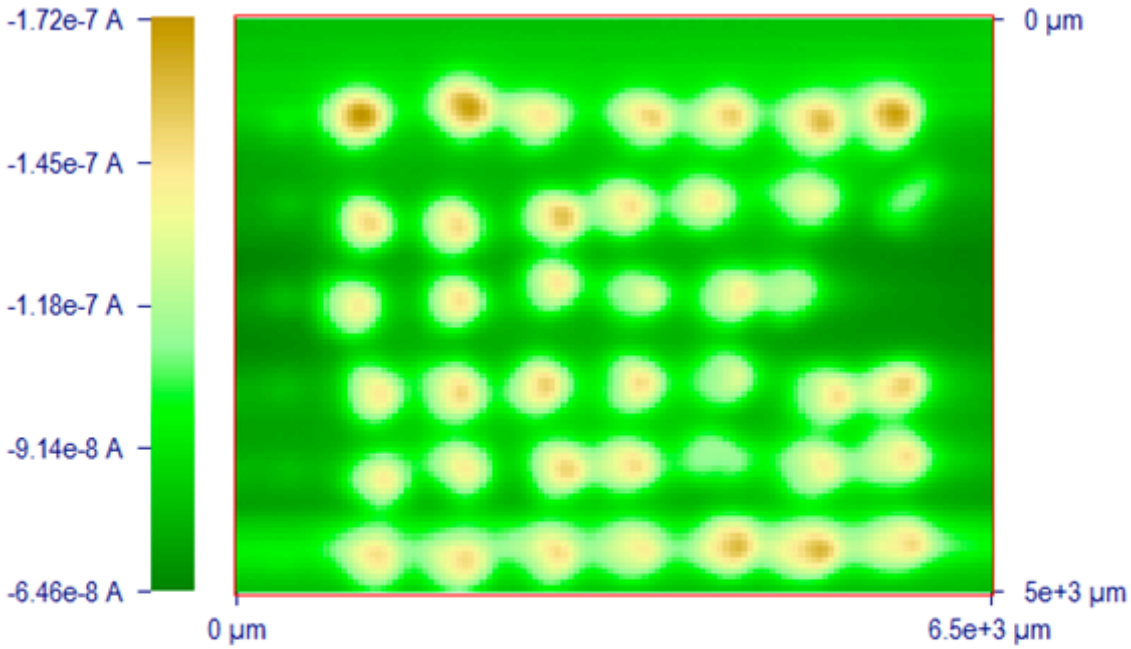

Figure S1. (b) SPECM images of the array photocurrent of Cu and Ni doped Bi/W oxide photocatalyst in a 0.1 M Na_2SO_3/Na_2SO_4 solution with the array held at constant applied potential of 0.2 V (vs. Ag/AgCl reference electrode) under UV-visible light. The arrays show 'insignificant effect' of the dopants.

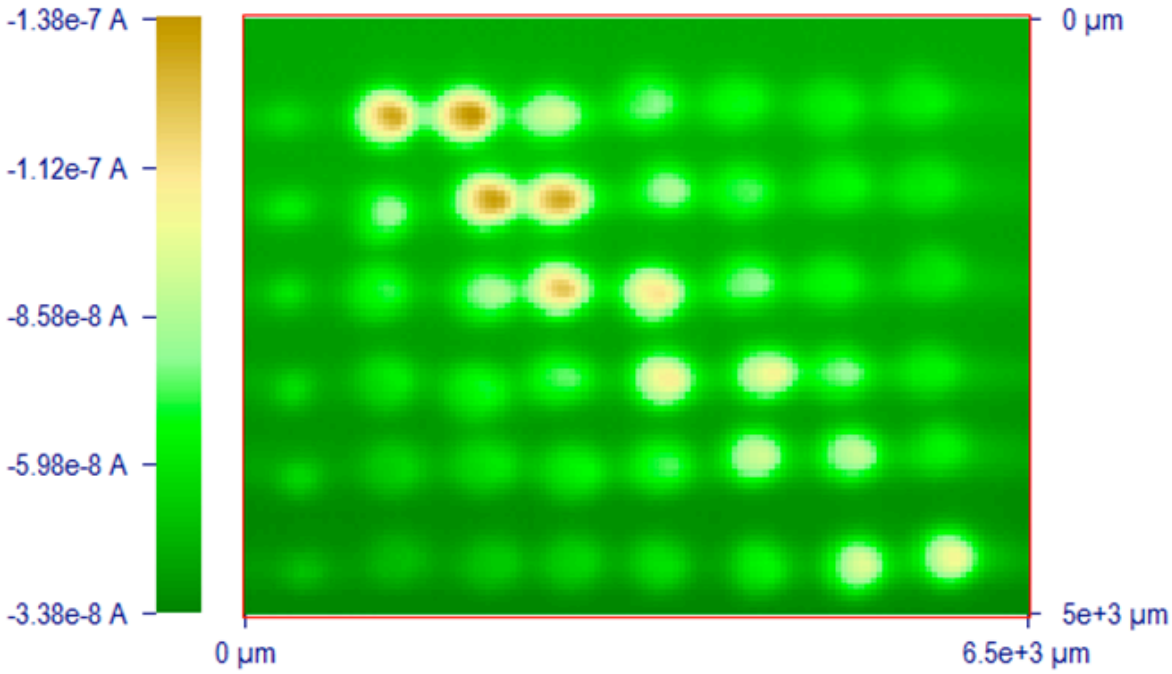

Figure S1. (c) SPECM images of the array photocurrent of Cr and Fe doped Bi/W oxide photocatalyst in a 0.1 M Na_2SO_3/Na_2SO_4 solution with the array held at constant applied potential of 0.2 V (vs. Ag/AgCl reference electrode) under UV-visible light. The arrays show 'negative effect' of the dopants.

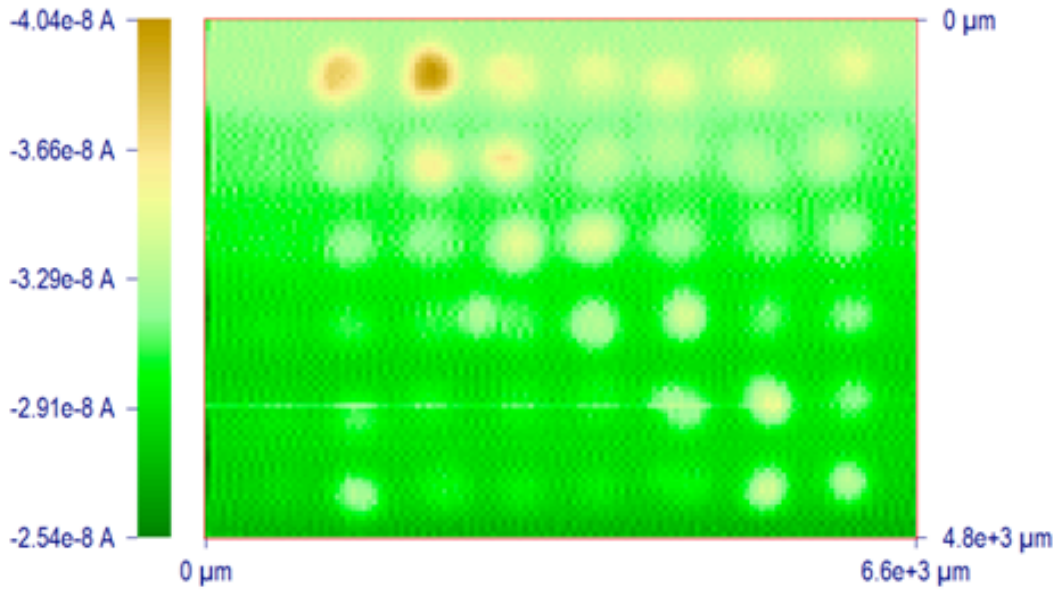

Figure S1. (d) SPECM images of the array photocurrent of Ag and Mo doped Bi/W oxide photocatalyst in a 0.1 M Na_2SO_3/Na_2SO_4 solution with the array held at constant applied potential of 0.2 V (vs. Ag/AgCl reference electrode) under UV-visible light. The arrays show 'negative effect' of the dopants.

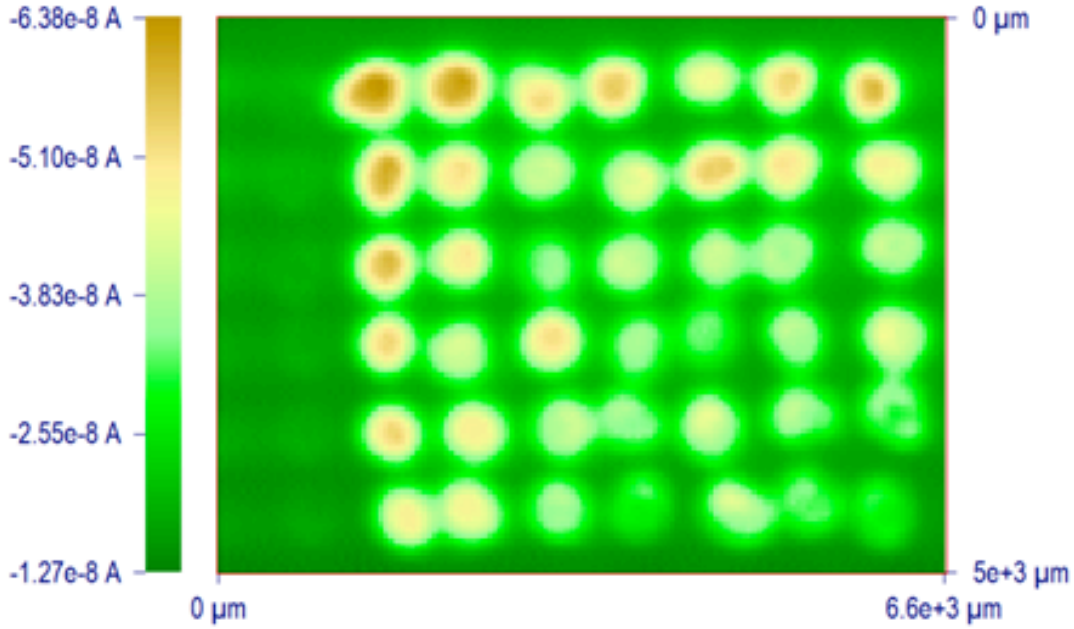

Figure S1. (e) SPECM images of the array photocurrent of Ca and Ta doped Bi/W oxide photocatalyst in a 0.1 M Na_2SO_3/Na_2SO_4 solution with the array held at constant applied potential of 0.2 V (vs. Ag/AgCl reference electrode) under UV-visible light. The arrays show 'insignificant effect' of the dopants.

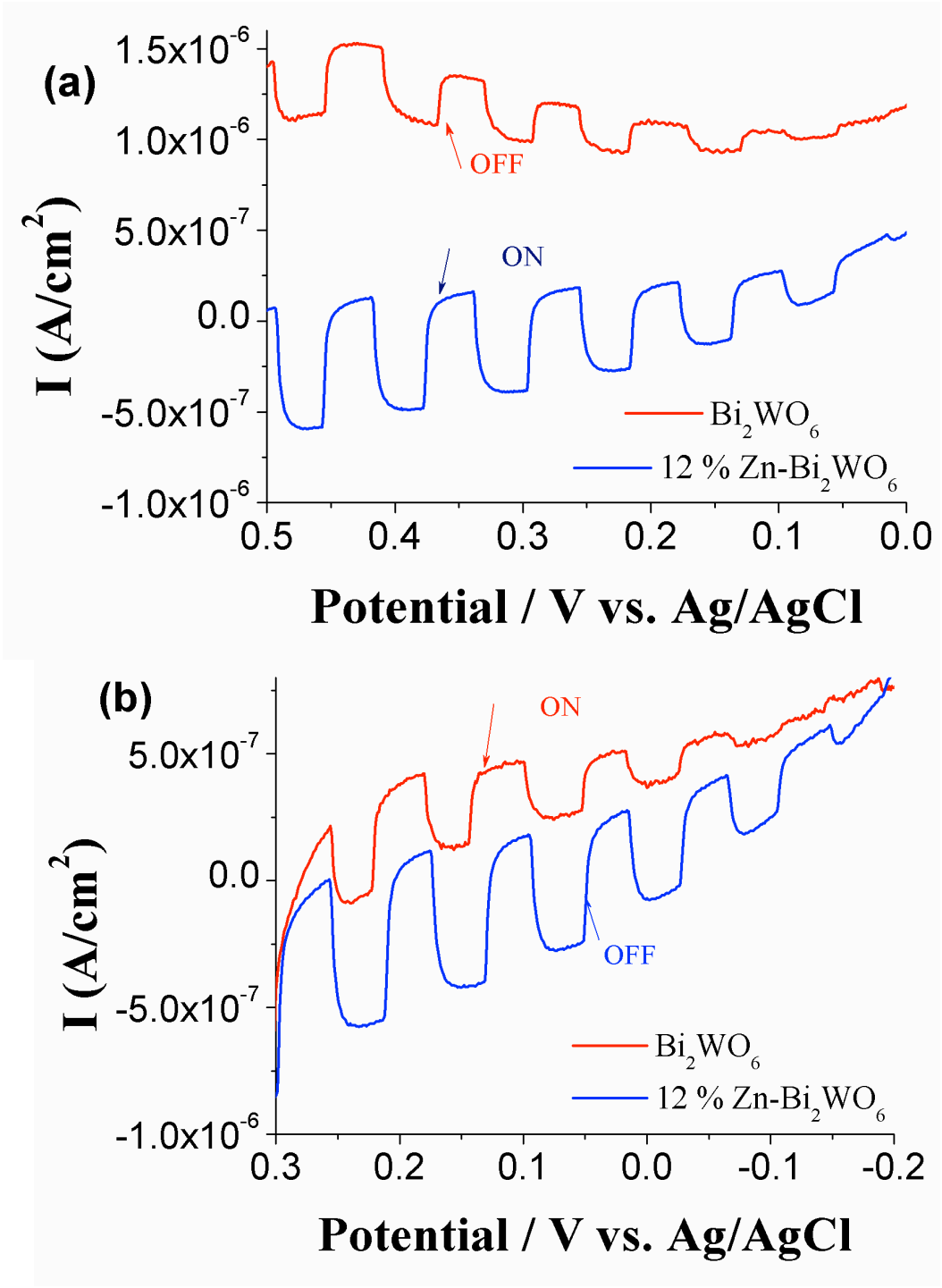

Figure S2. Linear sweep voltammograms (LSVs) of Bi_2WO_6 and 12% Zn doped Bi_2WO_6 thin films in (a) 0.1 M Na_2SO_4 (0.1M phosphate buffer) and (b) 0.1 M Na_2SO_3 with 0.1 M Na_2SO_4 solution under visible light illumination.

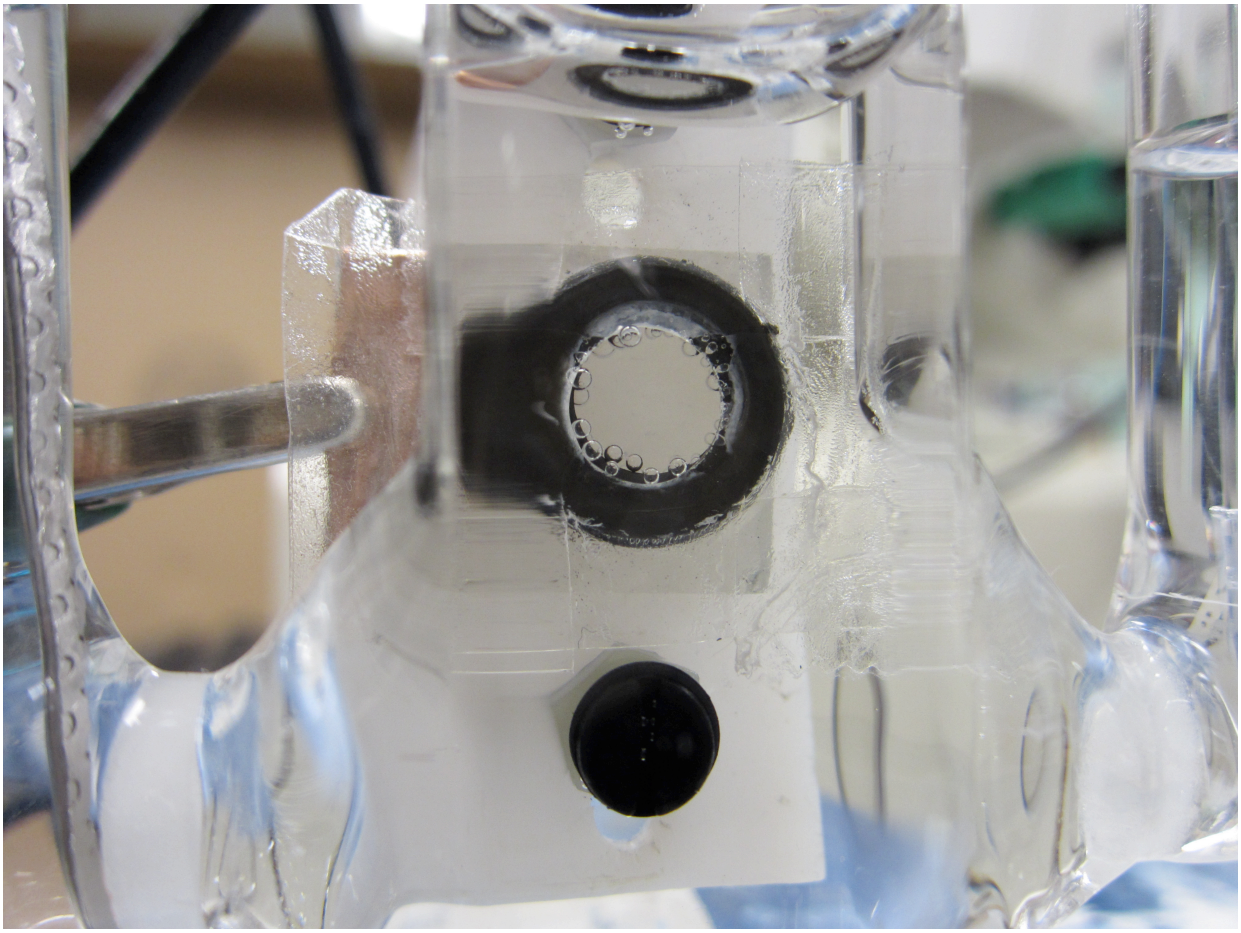

Figure S3. Photoelectrochemical water oxidation process: Oxygen bubble detected on the semiconductor surface through the rubber O-ring during chronoamperometry (stability test).

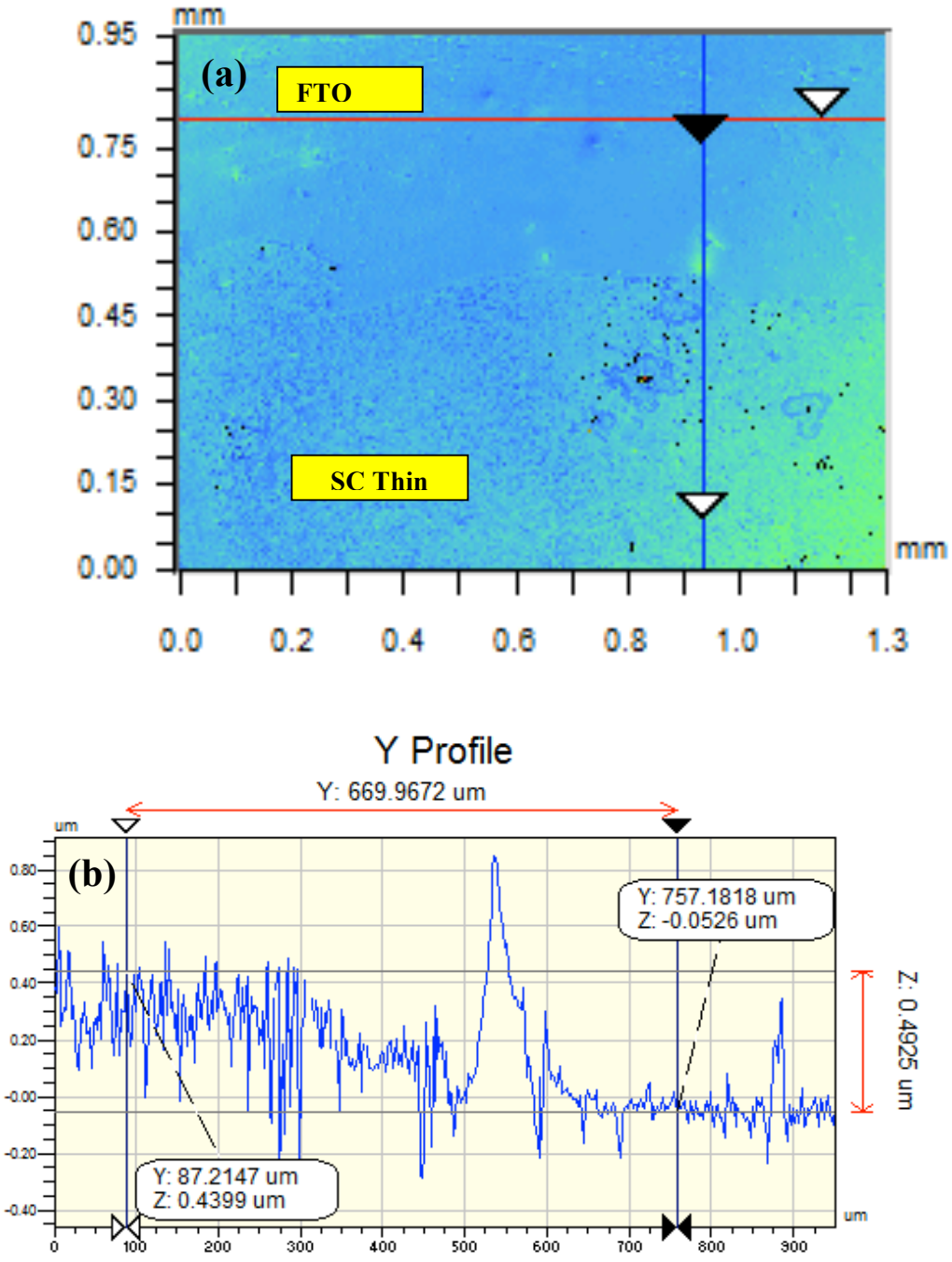

Figure S4. (a) Optical micrograph of the Bi_2WO_6 semiconductor film surface obtained through Veeco profiler. (b) Thickness profile diagram from FTO to oxide thin film (along Y axis).

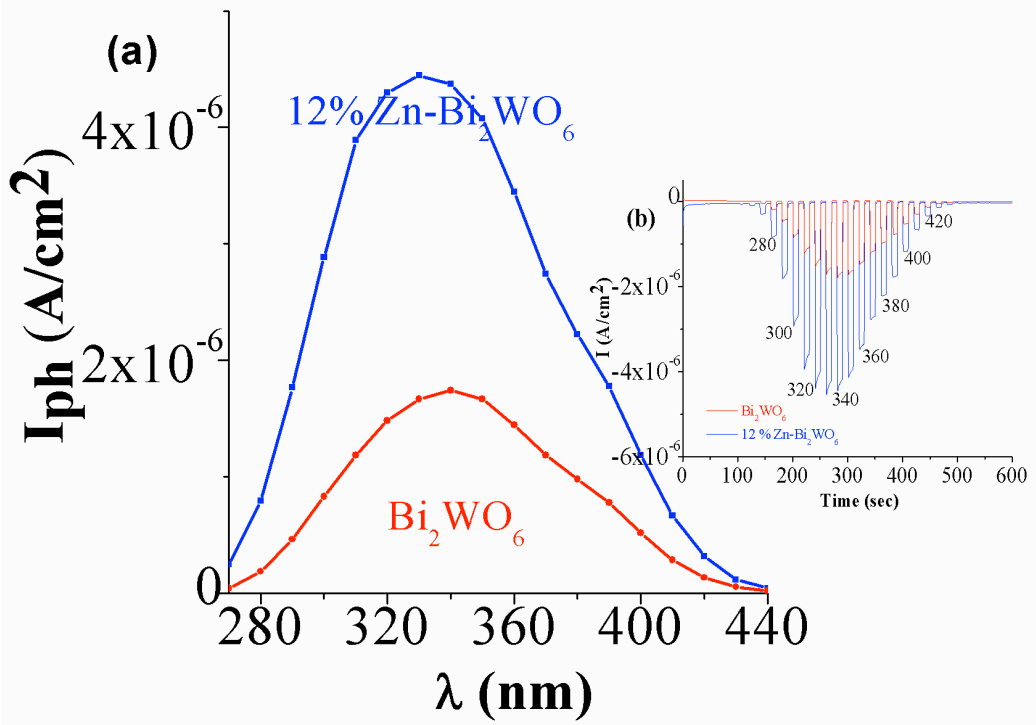

Figure S5. (a) Action spectrum of Bi_2WO_6 and 12% Zn doped Bi_2WO_6 thin films in 0.1 M SO_4^{2-} (0.1M phosphate buffer) solution. Constant applied potential 0.3 V vs. Ag/AgCl reference electrode. (b) Chronoamperometry plots with chopped monochromatic light at different wavelengths for the two materials in 0.1 M SO_4^{2-} (0.1M phosphate buffer) solutions to derive the action spectrum.

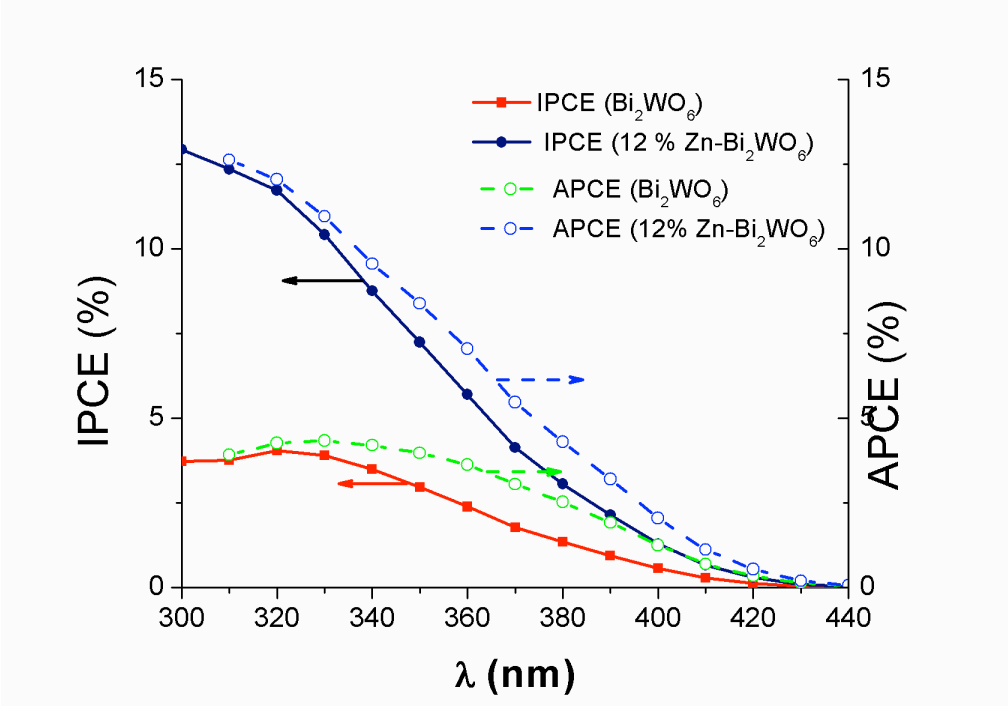

Figure S6. IPCE and APCE plots of Bi_2WO_6 and 12% Zn doped Bi_2WO_6 thin films in 0.1 M Na_2SO_4 (0.1M phosphate buffer) solution at applied potential 0.3 V vs. Ag/AgCl reference electrode.

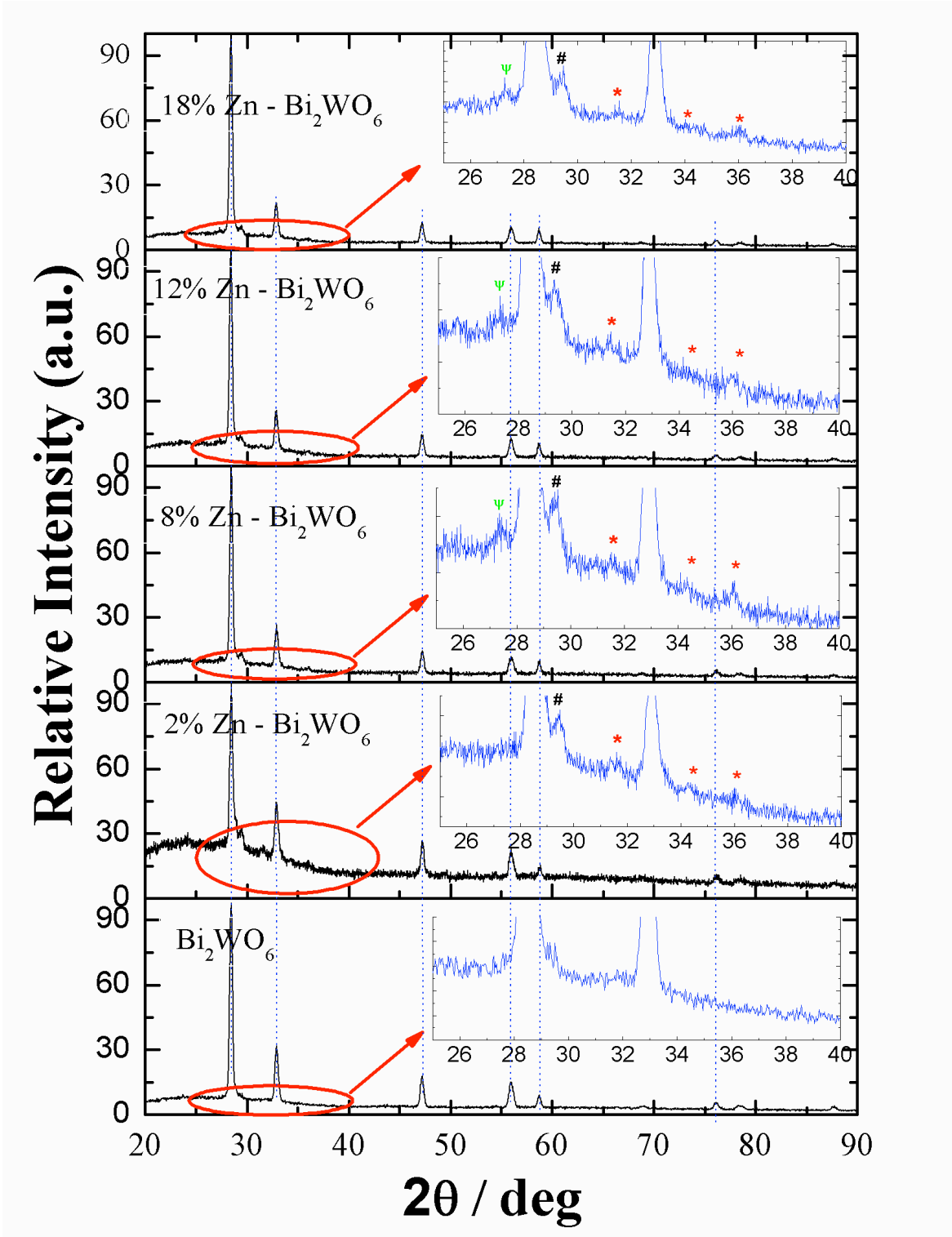

Figure S7. XRD pattern of the undoped Bi_2WO_6 and different level of Zn doped (2%, 8%, 12% and 18% Zn) Bi_2WO_6 thin films. The inset figures are magnified area under the curve, for identification of the low intense Bi_2O_3 and ZnO peaks. The different peaks marked as **ψ** : $Bi_2O_3^{cubic}$ - (index number: 16-0654); # : $Bi_2O_3^{cubic}$ - (index number: 65-3319) and * : $ZnO^{hexagonal}$ - (index number: 36-1451).